

# Electron interactions with Ar clusters and liquid Ar

**Francisco Blanco<sup>1</sup> and Gustavo García<sup>2,3</sup>**

<sup>1</sup>Departamento de Física Atómica Molecular y Nuclear, Facultad de Ciencias Físicas, Universidad Complutense de Madrid, Ciudad Universitaria, 28040 Madrid, Spain

<sup>2</sup>Instituto de Física Fundamental, Consejo Superior de Investigaciones Científicas, Serrano 113-bis, 28006 Madrid, Spain

<sup>3</sup>Centre for Medical Radiation Physics, University of Wollongong, NSW 2522, Australia

[g.garcia@iff.csic.es](mailto:g.garcia@iff.csic.es)

**Abstract.** Differential and integral electron scattering cross section from some Ar clusters (dimer, trimer and tetramer) are calculated for incident energies ranging from 1 to 500 eV by using a screening corrected additivity rule based on an independent atom representation (IAM-SCAR). The possibility of using this method to derive electron scattering cross section in the liquid phase is discussed and electron scattering cross section data for Ar liquid are provided.

## 1. Introduction

Secondary electrons have been proved to be responsible for the energy deposition pattern and related damage when irradiating matter with different high energy particles (photons, electrons, positrons or ions). Depending on the type and energy of primary radiation these electrons can be generated over a broad energy range from nearly zero up to the high energy of the primary particle (in the case of photoelectrons). Energy deposition models including secondary electron effects are required by some medical applications of radiations in the fields of radiotherapy, radiodiagnostics and radiation protection. One of the main difficulties to develop these models is that the subject targets are usually in the condensed phase, liquid or solid, while available cross section data are related to single atoms or molecules. The main goal of this paper is to study how target condensation can affect to the calculated electron scattering cross sections. We have chosen Ar for being a single atom with abundant cross section data available in the literature. In addition accurate theoretical and experimental cluster geometrical configurations for its dimer, trimer and tetramer have been recently published [1,2]. This allows us to apply our screening corrected additivity rule (SCAR) [3-6] to an independent atom representation (IAM) in order to follow the evolution of the differential (DCS) and integral (ICS) scattering cross section as a function of the number of atoms forming the cluster. This can be regarded as the way that atom condensation affects to the single atom scattering cross sections. Finally we can model the liquid state as a large cluster by assuming a homogeneous atom distribution defined by its density.

In this study we use the above mentioned IAM-SCAR method to calculate differential and integral electron scattering cross section for the Ar atom and its dimer, trimer and tetramer cluster configurations providing a systematic of the cross section value evolution as a function of the number of atoms in the cluster. We also present an approach to model electron scattering processes in liquid



Content from this work may be used under the terms of the [Creative Commons Attribution 3.0 licence](#). Any further distribution of this work must maintain attribution to the author(s) and the title of the work, journal citation and DOI.

argon by using this modified independent atom representation. The applicability of the present electron scattering data to model electron transport in liquids is finally discussed.

## 2. Calculation procedure

To describe the electron Ar scattering process an optical potential method has been followed. Both the potential and the calculation procedure have been extensively described elsewhere [3-5] and therefore only a brief summary will be reported here.

We represent the atomic target by an interacting complex potential (i.e. the optical potential), whose real part accounts for the elastic scattering of the incident electrons, while the imaginary part represents the inelastic processes that are considered as ‘absorptions’ from the incident beam. To construct this complex potential for each atom, the real part of the potential is represented by the sum of three terms: (i) a static term derived from a Hartree-Fock calculation of the atomic charge distribution [6], (ii) an exchange term to account for the indistinguishability of the incident and target electrons [7] and (iii) a polarisation term [8] for the long-range interactions which depend on the target dipole polarisability [9]. The imaginary part, following the procedure of Staszewska et al.[10], then treats inelastic scattering as electron–electron collisions. However, we initially found some major discrepancies in the available scattering data, which were subsequently corrected when a physical formulation of the absorption potential [3] was introduced. Further improvements to the original formulation, such as the inclusion of screening effects, local velocity corrections and in the description of the electrons’ indistinguishability [4], finally led to a model that provides a good approximation of electron–atom scattering over a broad energy range. An excellent example of this was for elastic electron–atomic iodine (I) scattering [11], where the optical potential results compared very favourably with those from an independent highly sophisticated Dirac-B-spline R-matrix computation.

### 2.1. Ar dimer, trimer and tetramer electron scattering calculation

To calculate the cross sections for electron scattering from Ar clusters, we follow the IAM, in the same way it is used for molecules [4], by applying what is commonly known as the additivity rule (AR). In this approach, the cluster scattering amplitude is derived from the sum of all the relevant atomic amplitudes, including the phase coefficients, which lead to the cluster DCSs for the atomic structure in question.

Integral cross sections (ICS) can then be determined by integrating those DCSs. The sum of the elastic and the absorption (for all inelastic processes except rotations and vibrations) gives the TCSs. Alternatively, the ICSs for the cluster can also be derived from the relevant atomic ICSs in conjunction with the optical theorem [4]. We found an inherent contradiction in the original formulation of the AR procedure between the ICSs derived from those two approaches, which suggested that the optical theorem was being violated [12]. This problem has been resolved by employing a normalization procedure during the calculation of the DCSs which ensures that the ICSs derived from the two approaches are now entirely consistent [12]. An additional limitation of the AR method is that no target structure is considered, so that it is really only applicable when the incident electrons are so fast that they effectively see the target cluster as a sum of individual atoms (typically above  $\sim 100$  eV). To reduce this limitation, we [13, 14] introduced the SCAR method, which considers the geometry of a relevant atomic structure (atomic positions and bond lengths) by using some screening coefficients. With this correction the range of validity of the IAM-SCAR approach might be extended to incident electron energies of about 20 eV. Indeed it is the elastic DCS and the elastic and inelastic ICS results from the application of the IAM-SCAR method to Ar dimer, trimer and tetramer that we report on here. Atomic positions and bond lengths for these clusters have been taken from [1].

### 2.2. Liquid Ar electron scattering calculation

We can consider a liquid as formed by a homogeneous mixture of atoms which interatomic distances are given by its temperature and density conditions ( $1430 \text{ kg/m}^3$  in the case of Ar). By assuming that

the screening corrections are not very dependent on the direction of the incident electrons we can apply the SCAR procedure, in a similar way we accomplished for molecules and clusters, in order to calculate the effective cross section ( $\sigma_i^{\text{eff}}$ ) of an Ar atom within the liquid. A sketch of the screening situation for different electron energies is shown in Figure 1. For high energies electrons (a), above 100 eV, where atomic electron scattering cross sections do not overlap, an independent atom representation of the solid is appropriate. However, for intermediate energies (b), between 20 and 100 eV, overlapping between atomic cross sections occur and the effective cross section of the  $i$  atom ( $\sigma_i^{\text{eff}}$ ) is less than the atomic cross section ( $\sigma_i$ ) by the  $\sigma_{ij}$  screening coefficients provided by the  $j$  surrounding atoms. At low energies (c), below 20 eV, the effective cross section approaches to the cell size  $\sigma^{\text{eff}} = \sigma^c$ .

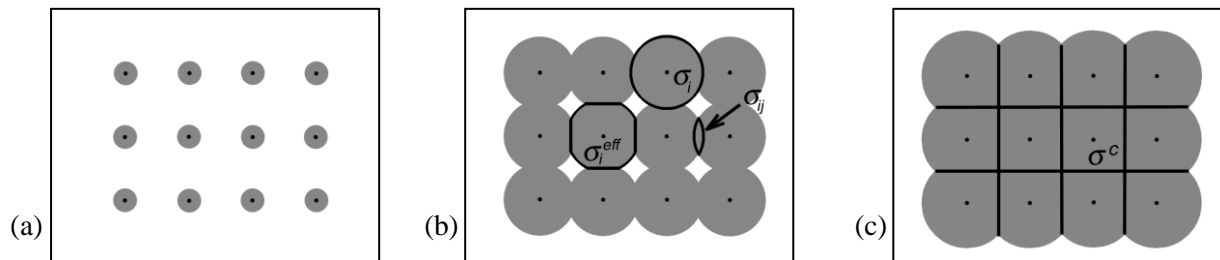


**FIGURE 1.** Geometric representation of the Ar atomic cross section for (a) high, (b) intermediate and (c) low incident energy electrons

### 3. Results and discussion

Differential electron elastic scattering cross section for Ar atom, dimer, trimer and tetramer are shown in Table 1 and plotted in Figure 2 for selected energies ranging from 1 to 1000 eV. By integrating over the whole scattering angle range we derived the corresponding integral elastic cross sections which, in conjunction with the optical theorem, provided the total scattering cross sections and therefore, the integral inelastic cross sections. Integral electron scattering cross sections for Ar atoms and Ar clusters are shown in Table 2. Due to the small binding energy of these Ar clusters, a few meV, and their relatively large internuclear distances we can expect no much different scattering behavior from that of the independent atoms for the energy range considered here. However, it has been recently shown [14] that the multicenter structure of small noble gas clusters modifies the electron impact ionization dynamics even for incident energies of 100 eV.

**TABLE 1.** Differential electron scattering cross sections from Argon atoms ( $\text{Ar}_1$ ) and Argon clusters ( $\text{Ar}_2$ ,  $\text{Ar}_3$ ,  $\text{Ar}_4$ ), in atomic units ( $a_0^2/\text{Sr}$ ), for selected energies.

Ang (deg)	1 eV				10 eV				100 eV			
	$\text{Ar}_1$	$\text{Ar}_2$	$\text{Ar}_3$	$\text{Ar}_4$	$\text{Ar}_1$	$\text{Ar}_2$	$\text{Ar}_3$	$\text{Ar}_4$	$\text{Ar}_1$	$\text{Ar}_2$	$\text{Ar}_3$	$\text{Ar}_4$
0	0.0917	0.193	0.305	0.432	33.4	86.6	153	229	50	144	278	451
1	0.0906	0.191	0.301	0.427	33.2	86	152	227	48.4	138	267	431
2	0.0874	0.184	0.291	0.412	32.6	84.3	149	222	45.4	127	244	391
3	0.0823	0.173	0.275	0.389	31.9	82.1	145	216	42.7	116	219	347
4	0.0757	0.16	0.253	0.36	31.1	79.8	141	209	40.1	105	193	301
5	0.068	0.144	0.229	0.325	30.3	77.6	136	202	37.5	93.6	166	254

6	0.0597	0.127	0.202	0.287	29.7	75.3	132	195	35.1	82.8	142	210
7	0.0512	0.109	0.174	0.249	29	73	128	188	32.8	72.8	119	170
8	0.0429	0.092	0.148	0.212	28.2	70.7	123	181	30.5	63.9	99.4	136
9	0.0353	0.0763	0.123	0.178	27.5	68.3	118	173	28.4	56.1	83	108
10	0.0286	0.0624	0.102	0.147	26.8	65.9	113	165	26.3	47.6	63.5	73.1
11	0.023	0.0507	0.0835	0.122	26.1	63.5	108	158	24.3	40.4	48.4	47.8
12	0.0186	0.0416	0.0693	0.102	25.5	61.2	104	150	22.4	35.2	38.7	33.1
13	0.0154	0.0351	0.0591	0.0879	24.8	58.8	98.9	142	20.6	31.6	33.5	26.9
14	0.0136	0.0313	0.0532	0.0797	24.1	56.4	94.2	135	18.9	29.2	31.5	26.8
15	0.0131	0.0303	0.0517	0.0775	23.4	54.1	89.5	127	17.3	27.6	31.7	30.6
16	0.014	0.0321	0.0544	0.0813	22.8	51.8	84.9	120	15.8	26.5	32.9	36.1
17	0.0162	0.0366	0.0615	0.0912	22.1	49.6	80.4	113	14.4	25.6	34.4	41.7
18	0.0198	0.0441	0.0731	0.107	21.4	47.4	76.1	106	13.1	24.7	35.4	46.1
19	0.0248	0.0545	0.0892	0.13	20.8	45.2	71.8	99.1	11.8	23.3	34.7	46.3
20	0.0314	0.0679	0.11	0.159	20.2	43.1	67.7	92.6	10.6	21.4	32.5	44.1
21	0.0394	0.0845	0.136	0.194	19.5	41.1	63.8	86.4	9.55	19.6	30.1	41.2
22	0.0489	0.104	0.166	0.237	18.9	39.2	60	80.5	8.55	17.7	27.4	37.7
23	0.0599	0.127	0.201	0.285	18.3	37.3	56.4	74.9	7.63	15.8	24.5	33.7
24	0.0724	0.152	0.241	0.34	17.7	35.5	53	69.6	6.78	14	21.6	29.5
25	0.0862	0.18	0.284	0.401	17.1	33.7	49.7	64.6	6.01	12.3	18.8	25.3
26	0.101	0.211	0.332	0.467	16.5	32.1	46.7	60	5.3	10.7	16.1	21.5
27	0.117	0.245	0.383	0.538	15.9	30.5	43.8	55.6	4.66	9.27	13.8	18
28	0.135	0.28	0.438	0.613	15.3	29	41.1	51.6	4.08	7.99	11.6	14.7
29	0.153	0.317	0.495	0.692	14.8	27.6	38.6	47.9	3.57	6.75	9.48	11.6
30	0.171	0.355	0.554	0.774	14.3	26	35.4	42.3	3.11	5.71	7.78	9.24
31	0.191	0.395	0.615	0.857	13.7	24.3	32.1	37	2.69	4.85	6.47	7.54
32	0.21	0.435	0.677	0.943	13.2	22.7	29	32.2	2.33	4.15	5.48	6.37
33	0.231	0.476	0.74	1.03	12.7	21.3	26.3	28.1	2.01	3.58	4.75	5.59
34	0.251	0.518	0.804	1.12	12.2	20	23.9	24.5	1.73	3.11	4.19	5.07
35	0.272	0.56	0.869	1.21	11.8	18.8	21.9	21.5	1.48	2.71	3.75	4.68
36	0.293	0.602	0.934	1.3	11.3	17.7	20	18.9	1.26	2.38	3.38	4.36
37	0.313	0.645	0.999	1.39	10.9	16.7	18.5	16.8	1.08	2.09	3.05	4.05
38	0.334	0.687	1.06	1.47	10.5	15.9	17.2	15.1	0.922	1.82	2.7	3.61
39	0.355	0.73	1.13	1.56	10.1	15.1	16	13.7	0.785	1.57	2.36	3.17
40	0.376	0.771	1.19	1.65	9.69	14.4	15.1	12.7	0.669	1.35	2.05	2.77
41	0.396	0.813	1.25	1.73	9.32	13.7	14.3	11.9	0.571	1.16	1.77	2.4
42	0.416	0.853	1.32	1.82	8.98	13.2	13.7	11.4	0.488	0.996	1.52	2.07
43	0.436	0.893	1.38	1.9	8.64	12.7	13.3	11.1	0.418	0.855	1.31	1.77
44	0.455	0.931	1.43	1.98	8.33	12.3	12.9	10.9	0.36	0.736	1.12	1.51
45	0.473	0.968	1.49	2.05	8.03	11.9	12.6	11	0.313	0.636	0.966	1.29
46	0.491	1	1.54	2.13	7.75	11.6	12.4	11.1	0.274	0.554	0.836	1.11
47	0.508	1.04	1.6	2.19	7.48	11.3	12.3	11.4	0.242	0.488	0.731	0.964
48	0.524	1.07	1.64	2.26	7.24	11	12.3	11.7	0.217	0.433	0.639	0.825
49	0.54	1.1	1.69	2.32	7	10.8	12.3	12.1	0.198	0.388	0.566	0.721
50	0.555	1.13	1.74	2.39	6.78	10.6	12.3	12.6	0.184	0.356	0.513	0.649
51	0.57	1.16	1.78	2.44	6.58	10.5	12.4	13.1	0.173	0.333	0.476	0.602

52	0.584	1.19	1.82	2.5	6.4	10.4	12.6	13.6	0.167	0.319	0.456	0.579
53	0.597	1.22	1.86	2.55	6.22	10.2	12.7	14.1	0.163	0.312	0.448	0.575
54	0.61	1.24	1.9	2.6	6.05	10.1	12.8	14.7	0.162	0.312	0.452	0.588
55	0.623	1.27	1.94	2.65	5.9	10.1	13	15.2	0.164	0.318	0.466	0.616
56	0.635	1.29	1.97	2.7	5.77	10	13.2	15.8	0.167	0.328	0.488	0.655
57	0.647	1.31	2.01	2.74	5.64	9.96	13.4	16.3	0.172	0.343	0.517	0.704
58	0.658	1.34	2.04	2.78	5.52	9.92	13.6	16.8	0.179	0.361	0.548	0.745
59	0.668	1.36	2.07	2.82	5.41	9.89	13.7	17.3	0.186	0.379	0.578	0.787
60	0.678	1.38	2.1	2.86	5.32	9.87	13.9	17.8	0.195	0.398	0.61	0.833
61	0.688	1.39	2.12	2.89	5.22	9.85	14.1	18	0.205	0.42	0.644	0.879
62	0.696	1.41	2.15	2.92	5.14	9.77	14	18	0.216	0.442	0.679	0.925
63	0.704	1.43	2.17	2.95	5.06	9.69	14	18	0.227	0.465	0.713	0.968
64	0.712	1.44	2.19	2.98	4.99	9.61	13.9	18	0.239	0.488	0.746	1.01
65	0.719	1.45	2.21	3	4.92	9.52	13.9	18	0.251	0.512	0.778	1.05
66	0.725	1.47	2.23	3.02	4.85	9.44	13.8	18	0.264	0.535	0.809	1.08
67	0.731	1.48	2.24	3.04	4.79	9.37	13.7	18	0.277	0.557	0.838	1.11
68	0.736	1.49	2.25	3.05	4.73	9.29	13.7	17.9	0.29	0.58	0.866	1.13
69	0.74	1.49	2.27	3.07	4.67	9.21	13.6	17.9	0.303	0.601	0.886	1.14
70	0.744	1.5	2.28	3.08	4.61	9.12	13.5	17.8	0.316	0.619	0.901	1.15
71	0.747	1.51	2.28	3.09	4.55	9.04	13.4	17.7	0.329	0.637	0.918	1.16
72	0.75	1.51	2.29	3.09	4.5	8.95	13.3	17.6	0.341	0.655	0.938	1.18
73	0.752	1.51	2.29	3.09	4.43	8.85	13.2	17.4	0.354	0.675	0.962	1.22
74	0.753	1.52	2.29	3.09	4.37	8.74	13.1	17.3	0.366	0.695	0.991	1.26
75	0.754	1.52	2.29	3.09	4.31	8.63	12.9	17.1	0.377	0.717	1.02	1.31
76	0.753	1.52	2.29	3.08	4.24	8.51	12.7	16.8	0.388	0.74	1.06	1.38
77	0.752	1.51	2.28	3.07	4.17	8.37	12.5	16.6	0.398	0.763	1.11	1.45
78	0.75	1.51	2.27	3.06	4.09	8.23	12.3	16.3	0.407	0.787	1.15	1.53
79	0.747	1.5	2.26	3.04	4.02	8.08	12.1	16	0.415	0.81	1.2	1.61
80	0.743	1.49	2.25	3.02	3.93	7.91	11.8	15.6	0.422	0.832	1.24	1.66
81	0.738	1.48	2.23	3	3.84	7.73	11.6	15.3	0.428	0.85	1.27	1.7
82	0.733	1.47	2.22	2.97	3.75	7.54	11.3	14.9	0.433	0.864	1.3	1.74
83	0.727	1.46	2.2	2.94	3.65	7.34	11	14.5	0.437	0.875	1.32	1.77
84	0.721	1.44	2.17	2.91	3.55	7.14	10.7	14	0.44	0.883	1.33	1.79
85	0.713	1.43	2.15	2.88	3.44	6.91	10.3	13.6	0.441	0.887	1.34	1.8
86	0.705	1.41	2.12	2.84	3.33	6.69	9.98	13.1	0.441	0.888	1.34	1.8
87	0.697	1.4	2.1	2.81	3.21	6.45	9.62	12.6	0.44	0.886	1.33	1.78
88	0.688	1.38	2.07	2.76	3.08	6.2	9.24	12.1	0.437	0.88	1.32	1.76
89	0.678	1.36	2.04	2.72	2.96	5.94	8.86	11.6	0.433	0.87	1.31	1.73
90	0.668	1.34	2.01	2.68	2.82	5.68	8.46	11.1	0.428	0.857	1.28	1.69
91	0.658	1.31	1.97	2.63	2.69	5.41	8.06	10.6	0.421	0.841	1.25	1.65
92	0.646	1.29	1.94	2.59	2.55	5.14	7.66	10	0.413	0.822	1.22	1.59
93	0.635	1.27	1.9	2.54	2.41	4.86	7.25	9.51	0.404	0.801	1.18	1.52
94	0.623	1.24	1.87	2.49	2.27	4.58	6.84	8.98	0.394	0.775	1.13	1.45
95	0.611	1.22	1.83	2.44	2.12	4.29	6.42	8.44	0.382	0.747	1.09	1.38
96	0.599	1.2	1.79	2.38	1.98	4.01	6.02	7.92	0.369	0.718	1.04	1.32
97	0.586	1.17	1.75	2.33	1.83	3.73	5.61	7.4	0.356	0.688	0.992	1.26

98	0.573	1.14	1.71	2.28	1.68	3.45	5.21	6.89	0.341	0.657	0.946	1.21
99	0.56	1.12	1.67	2.22	1.54	3.18	4.82	6.34	0.326	0.627	0.903	1.16
100	0.547	1.09	1.63	2.17	1.39	2.9	4.41	5.8	0.309	0.595	0.86	1.11
101	0.534	1.07	1.59	2.12	1.25	2.63	4.02	5.31	0.292	0.564	0.818	1.07
102	0.521	1.04	1.55	2.06	1.11	2.37	3.64	4.83	0.275	0.533	0.777	1.02
103	0.508	1.01	1.51	2.01	0.981	2.11	3.28	4.39	0.257	0.5	0.735	0.976
104	0.496	0.987	1.48	1.96	0.852	1.87	2.95	3.98	0.239	0.468	0.694	0.929
105	0.483	0.961	1.44	1.91	0.729	1.65	2.63	3.61	0.221	0.436	0.651	0.879
106	0.47	0.935	1.4	1.84	0.613	1.43	2.35	3.27	0.203	0.403	0.608	0.824
107	0.457	0.909	1.35	1.75	0.504	1.24	2.08	2.96	0.185	0.371	0.563	0.762
108	0.444	0.881	1.3	1.67	0.404	1.06	1.85	2.68	0.167	0.338	0.514	0.699
109	0.431	0.851	1.25	1.59	0.313	0.899	1.63	2.44	0.149	0.304	0.466	0.637
110	0.418	0.82	1.19	1.52	0.232	0.757	1.45	2.23	0.132	0.272	0.419	0.575
111	0.405	0.791	1.14	1.44	0.161	0.635	1.29	2.05	0.116	0.24	0.373	0.514
112	0.393	0.761	1.1	1.37	0.103	0.535	1.16	1.9	0.101	0.21	0.329	0.455
113	0.38	0.733	1.05	1.3	0.0567	0.456	1.06	1.79	0.086	0.182	0.287	0.399
114	0.368	0.705	1	1.24	0.0239	0.4	0.993	1.71	0.0726	0.155	0.247	0.347
115	0.355	0.678	0.958	1.18	0.00509	0.369	0.953	1.67	0.0604	0.131	0.211	0.299
116	0.343	0.651	0.915	1.12	0.0009	0.361	0.944	1.66	0.0495	0.11	0.179	0.256
117	0.331	0.625	0.873	1.06	0.012	0.38	0.967	1.68	0.0401	0.0912	0.151	0.219
118	0.319	0.6	0.833	1	0.039	0.425	1.02	1.75	0.0323	0.0757	0.128	0.188
119	0.307	0.575	0.794	0.95	0.0825	0.497	1.11	1.84	0.0262	0.0635	0.11	0.164
120	0.296	0.551	0.757	0.899	0.143	0.598	1.24	1.98	0.0219	0.055	0.0976	0.148
121	0.284	0.527	0.721	0.851	0.221	0.726	1.4	2.15	0.0196	0.0504	0.0906	0.138
122	0.273	0.504	0.686	0.804	0.316	0.885	1.59	2.37	0.0193	0.0497	0.0894	0.137
123	0.262	0.481	0.652	0.76	0.43	1.07	1.83	2.63	0.0211	0.0531	0.0943	0.142
124	0.251	0.459	0.619	0.717	0.562	1.29	2.1	2.93	0.0251	0.0608	0.105	0.156
125	0.24	0.438	0.587	0.676	0.713	1.54	2.41	3.27	0.0313	0.073	0.123	0.177
126	0.23	0.417	0.557	0.638	0.882	1.82	2.76	3.66	0.0399	0.0894	0.146	0.206
127	0.22	0.397	0.527	0.6	1.07	2.14	3.15	4.1	0.0509	0.11	0.175	0.243
128	0.209	0.377	0.499	0.565	1.28	2.48	3.59	4.59	0.0643	0.136	0.211	0.288
129	0.2	0.359	0.472	0.532	1.5	2.86	4.06	5.12	0.0801	0.166	0.254	0.341
130	0.19	0.34	0.446	0.5	1.75	3.27	4.58	5.72	0.0983	0.2	0.302	0.402
131	0.181	0.323	0.422	0.47	2.01	3.71	5.13	6.35	0.119	0.239	0.358	0.473
132	0.172	0.306	0.398	0.441	2.29	4.18	5.74	7.05	0.142	0.283	0.42	0.551
133	0.163	0.29	0.376	0.414	2.59	4.69	6.39	7.8	0.168	0.331	0.488	0.639
134	0.155	0.274	0.354	0.389	2.91	5.23	7.08	8.61	0.196	0.384	0.564	0.736
135	0.147	0.259	0.334	0.365	3.24	5.79	7.81	9.46	0.227	0.442	0.646	0.844
136	0.139	0.245	0.315	0.343	3.59	6.39	8.58	10.4	0.259	0.504	0.735	0.961
137	0.132	0.232	0.297	0.322	3.95	7.01	9.4	11.3	0.295	0.571	0.832	1.09
138	0.125	0.219	0.279	0.302	4.34	7.67	10.3	12.4	0.332	0.642	0.936	1.23
139	0.118	0.206	0.263	0.283	4.73	8.35	11.2	13.4	0.372	0.718	1.05	1.37
140	0.112	0.195	0.248	0.266	5.14	9.06	12.1	14.6	0.413	0.799	1.16	1.53
141	0.105	0.184	0.233	0.249	5.56	9.79	13.1	15.7	0.457	0.883	1.29	1.7
142	0.0994	0.173	0.219	0.234	5.99	10.5	14.1	17	0.502	0.972	1.42	1.88
143	0.0938	0.163	0.206	0.219	6.43	11.3	15.1	18.2	0.55	1.06	1.56	2.07

144	0.0885	0.154	0.194	0.206	6.89	12.1	16.2	19.6	0.598	1.16	1.7	2.27
145	0.0834	0.145	0.182	0.194	7.35	12.9	17.3	20.9	0.649	1.26	1.85	2.47
146	0.0787	0.136	0.172	0.182	7.82	13.8	18.4	22.3	0.701	1.36	2.01	2.68
147	0.0743	0.129	0.162	0.171	8.29	14.6	19.5	23.7	0.754	1.47	2.17	2.89
148	0.07	0.121	0.153	0.161	8.77	15.5	20.7	25.2	0.808	1.58	2.34	3.1
149	0.0661	0.114	0.144	0.152	9.25	16.3	21.9	26.7	0.863	1.69	2.5	3.32
150	0.0625	0.108	0.136	0.144	9.74	17.2	23.1	28.2	0.919	1.8	2.67	3.54
151	0.059	0.102	0.128	0.136	10.2	18.1	24.3	29.7	0.975	1.91	2.84	3.77
152	0.0558	0.0966	0.122	0.129	10.7	19	25.5	31.3	1.03	2.03	3	3.99
153	0.0528	0.0914	0.115	0.122	11.2	19.8	26.8	32.8	1.09	2.14	3.18	4.22
154	0.05	0.0866	0.109	0.116	11.7	20.7	28	34.4	1.14	2.25	3.34	4.44
155	0.0473	0.082	0.103	0.11	12.2	21.6	29.2	35.9	1.2	2.37	3.51	4.67
156	0.0448	0.0778	0.0982	0.104	12.6	22.5	30.4	37.5	1.26	2.48	3.68	4.89
157	0.0425	0.0738	0.0933	0.0995	13.1	23.3	31.6	39	1.31	2.59	3.84	5.11
158	0.0403	0.0701	0.0888	0.0949	13.6	24.2	32.8	40.5	1.37	2.7	4.01	5.33
159	0.0383	0.0667	0.0846	0.0907	14	25	33.9	42	1.42	2.81	4.17	5.54
160	0.0364	0.0636	0.0808	0.0868	14.4	25.8	35.1	43.5	1.48	2.91	4.33	5.75
161	0.0347	0.0607	0.0773	0.0833	14.9	26.6	36.2	44.9	1.53	3.02	4.49	5.96
162	0.0332	0.058	0.074	0.0801	15.3	27.3	37.3	46.3	1.58	3.12	4.64	6.16
163	0.0317	0.0556	0.0711	0.0771	15.7	28.1	38.3	47.7	1.63	3.22	4.78	6.35
164	0.0304	0.0534	0.0684	0.0745	16	28.8	39.3	49	1.67	3.31	4.92	6.53
165	0.0292	0.0514	0.066	0.0721	16.4	29.5	40.3	50.2	1.72	3.4	5.05	6.7
166	0.0281	0.0496	0.0638	0.0699	16.8	30.1	41.2	51.4	1.76	3.48	5.18	6.86
167	0.0272	0.0479	0.0619	0.068	17.1	30.7	42.1	52.6	1.8	3.56	5.3	7.02
168	0.0263	0.0465	0.0601	0.0662	17.4	31.3	42.9	53.6	1.84	3.64	5.41	7.17
169	0.0255	0.0451	0.0585	0.0647	17.7	31.8	43.7	54.6	1.87	3.71	5.52	7.31
170	0.0248	0.0439	0.057	0.0632	17.9	32.3	44.4	55.5	1.91	3.78	5.62	7.44
171	0.0241	0.0428	0.0557	0.062	18.2	32.8	45.1	56.4	1.94	3.84	5.71	7.56
172	0.0235	0.0419	0.0546	0.0609	18.4	33.2	45.6	57.2	1.97	3.89	5.79	7.66
173	0.023	0.041	0.0536	0.0598	18.6	33.6	46.2	57.8	1.99	3.94	5.86	7.76
174	0.0226	0.0403	0.0527	0.059	18.8	33.9	46.6	58.5	2.01	3.98	5.92	7.83
175	0.0222	0.0396	0.0519	0.0582	18.9	34.1	47	59	2.03	4.02	5.98	7.91
176	0.0219	0.0391	0.0513	0.0577	19	34.4	47.3	59.4	2.05	4.05	6.03	7.97
177	0.0216	0.0387	0.0508	0.0572	19.1	34.5	47.6	59.7	2.06	4.08	6.06	8.01
178	0.0214	0.0384	0.0504	0.0568	19.2	34.7	47.8	60	2.07	4.09	6.09	8.05
179	0.0213	0.0382	0.0502	0.0566	19.2	34.7	47.9	60.1	2.07	4.1	6.1	8.07
180	0.0213	0.0381	0.0501	0.0565	19.2	34.8	47.9	60.1	2.08	4.11	6.11	8.08

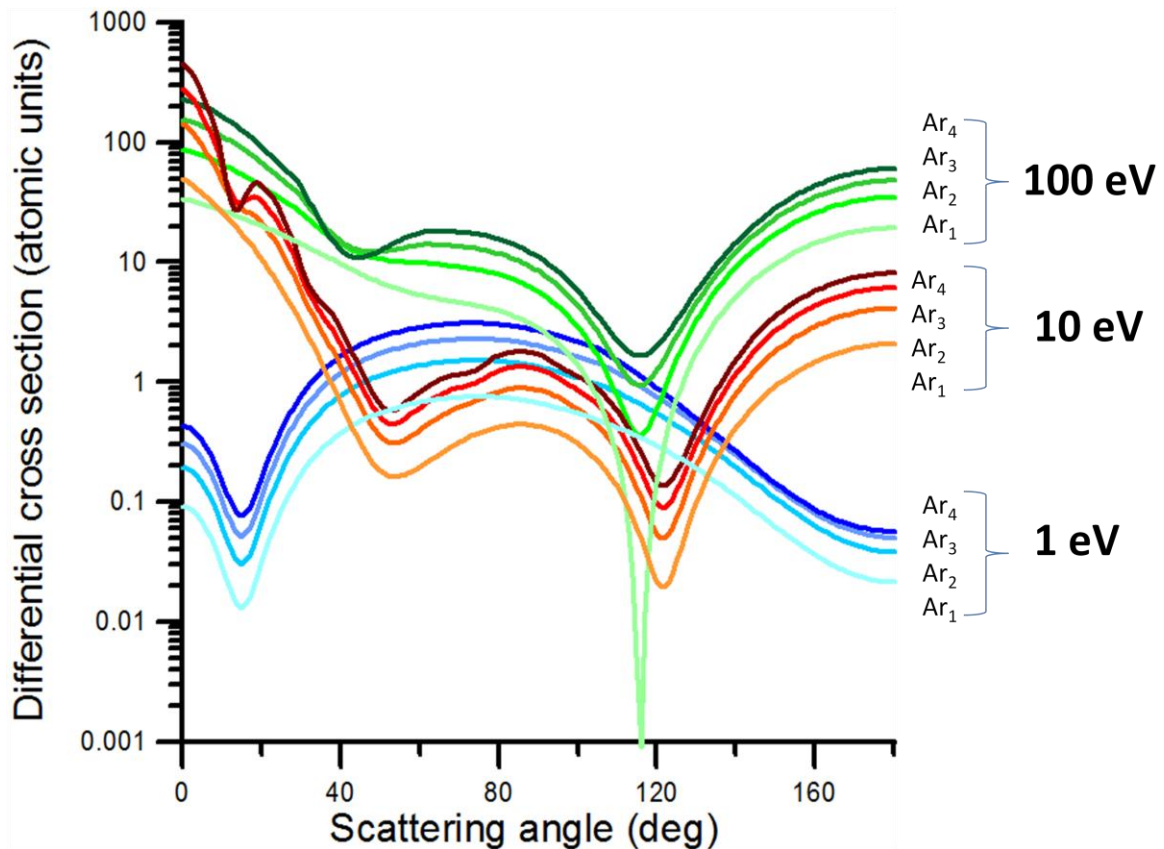


**FIGURE 2.** Differential electron scattering cross sections from Argon atoms ( $\text{Ar}_1$ ) and Argon clusters ( $\text{Ar}_2$ ,  $\text{Ar}_3$ ,  $\text{Ar}_4$ ), in atomic units ( $a_0^2/\text{Sr}$ ) for selected energies

**TABLE 2.** Integral elastic (ECS), inelastic (ICS) and total (TCS) electron scattering cross sections from Argon atoms ( $\text{Ar}_1$ ) and Argon clusters ( $\text{Ar}_2$ ,  $\text{Ar}_3$ ,  $\text{Ar}_4$ ), in atomic units ( $a_0^2$ ) for incident energies ranging from 1 to 500 eV

E(eV)	$\text{Ar}_1$			$\text{Ar}_2$			$\text{Ar}_3$			$\text{Ar}_4$		
	ECS	ICS	TCS									
1	5.39	0	5.39	10.7	0	10.7	16	0	16	21.3	0	21.3
1.5	11.3	0	11.3	22.5	0	22.5	33.4	0	33.4	44.2	0	44.2
2	16.9	0	16.9	33.3	0	33.3	49.3	0	49.3	64.9	0	64.9
3	26.2	0	26.2	51.4	0	51.4	75.5	0	75.5	98.8	0	98.8
4	33.8	0	33.8	65.9	0	65.9	96.4	0	96.4	125	0	125
5	40.7	0	40.7	78.8	0	78.8	115	0	115	148	0	148

7	53.5	0	53.5	103	0	103	148	0	148	189	0	189
10	72.2	0	72.1	136	0	136	193	0	193	245	0	245
15	83.2	0.235	83.5	156	0.44	156	219	0.62	220	275	0.778	276
20	71.9	2.47	74.4	136	4.65	140	192	6.59	199	243	8.34	251
30	48.2	6.67	54.9	92.3	12.8	105	133	18.4	151	170	23.6	194
40	35.6	8.4	44	68.9	16.2	85.1	99.9	23.5	123	129	30.4	159
50	28.6	9.11	37.7	55.5	17.7	73.2	80.9	25.8	107	105	33.5	138
70	21.1	9.41	30.5	41.1	18.4	59.5	60.3	26.9	87.2	78.7	35.1	114
100	15.9	9.03	24.9	31.2	17.7	48.9	45.9	26.1	72	60.1	34.1	94.2
150	12.1	8.12	20.2	23.8	16	39.8	35.1	23.6	58.7	46.2	31	77.2
200	10.2	7.32	17.5	20.1	14.4	34.6	29.8	21.4	51.2	39.3	28.2	67.4
300	8.19	6.15	14.3	16.2	12.2	28.4	24	18	42.1	31.7	23.8	55.5
400	7.02	5.33	12.4	13.9	10.6	24.5	20.7	15.7	36.4	27.3	20.7	48
500	6.23	4.72	11	12.4	9.36	21.7	18.4	13.9	32.3	24.3	18.4	42.7

In order to quantify the modification of the single atomic cross sections induced by the surrounding atoms we have evaluated the deviation of the cluster cross sections with those corresponding to the single atom multiplied by the number of atoms in the cluster. For the differential elastic scattering cross sections, these deviations, in percentage, are represented in Figure 3 as  $\text{deviation (\%)} = 100(\text{Ar}_n \cdot n\text{Ar}_1)/n\text{Ar}_1$ . As can be seen in this figure, for 1 eV incident energy there is a clear enhancement of the differential cross section for low angles, from  $0^\circ$  to about  $60^\circ$  with a clear maximum around  $15^\circ$ , while differential values clearly decrease for high angles above  $100^\circ$ . This behavior shows a clear interference pattern indicating how the cluster structure modifies the angular distribution of scattered electrons with respect to that given by isolated atoms.

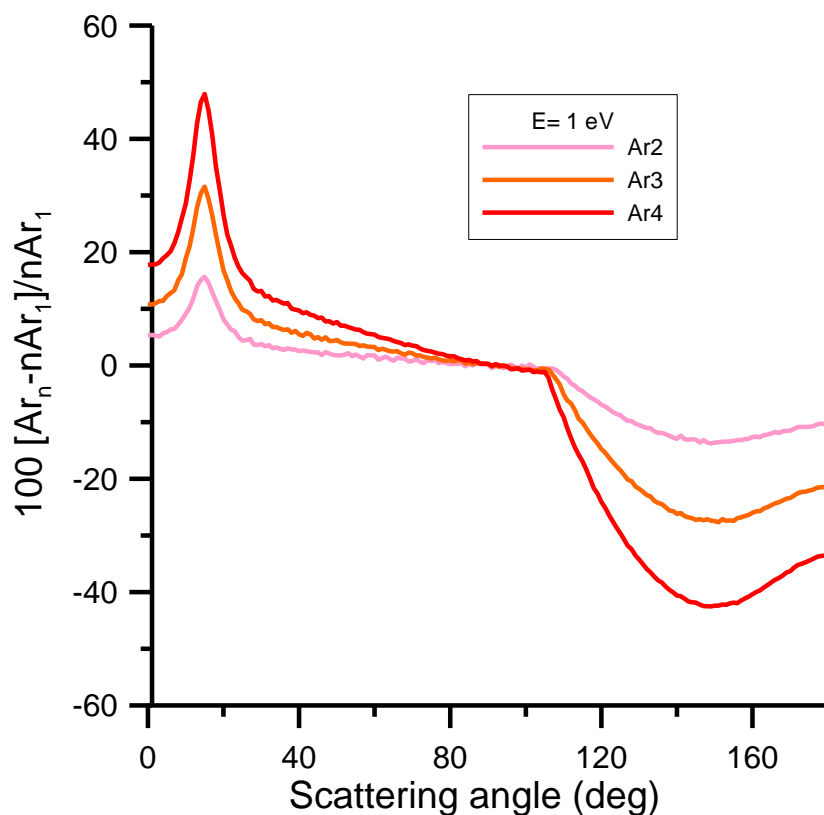


**FIGURE 3.** Percentage deviation of the differential elastic electron scattering cross section of  $\text{Ar}_n$  ( $n=2, 3, 4$ ) clusters with respect to the corresponding to isolated atoms for 1 eV incident energy.

Concerning integral cross sections, similar deviations have been plotted in Figure 4 for the total scattering cross sections of the Ar clusters with respect to those of isolated atoms. As seen from this figure, the total cross sections of clusters tend to be systematically lower than the corresponding to isolated atoms. For energies above 200 eV, these differences are nearly a constant factor. However, below these values, they tend to be quite energy dependent reaching the higher deviations around 15 eV

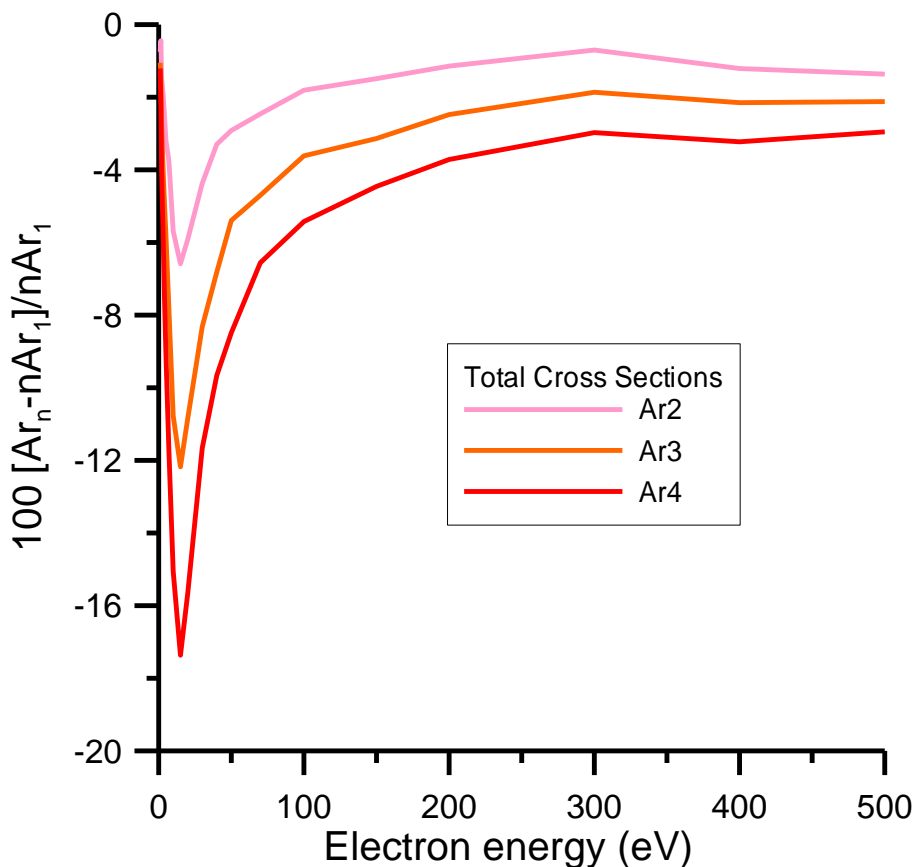


**FIGURE 4.** Percentage deviation of the total electron scattering cross section of  $\text{Ar}_n$  ( $n=2, 3, 4$ ) clusters with respect to the corresponding to isolated atoms

Finally integral electron scattering cross sections for liquid Ar derived with the procedure described above are shown in Figure 5. As expected from the tendency showed by the Ar clusters, the total scattering cross sections of Ar in the liquid state is lower than those for isolated Ar atoms. This decrement is a consequence of the multiple scattering with surrounding atoms and provides an indication of the relevance of condensation effects as a function of the incident energy. Although

multiple-scattering effects can be observed even at 100 eV [15], they are dominant at lower energies, between 3 and 40 eV, reaching their maximum contribution to the scattering processes around 15 eV.

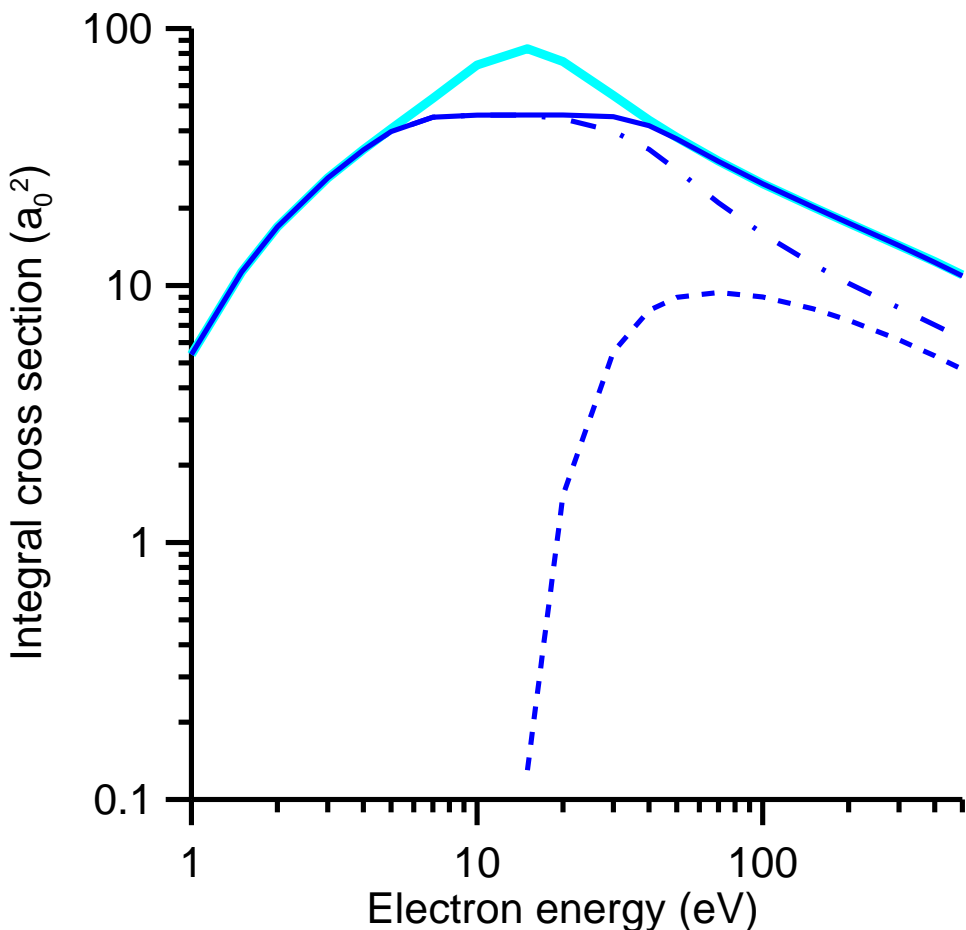


**FIGURE 5.** Integral cross sections (—, elastic, -·-, inelastic, —, total) for liquid Ar. The total cross sections for isolated Ar atoms (—) are also included for comparison

#### 4. Conclusions

The screening corrected additivity rule (SCAR) over an independent atom representation has been applied to calculate differential and integral electron scattering cross sections by Ar clusters (dimer, trimer and tetramer) for incident energies ranging from 1 to 500 eV. This calculation confirmed that, as observed by Plüger et al. [14], multiple scattering in the cluster produces a redistribution of the scattering angles and important changes on the integral cross sections with respect to those for the atomic Ar, even at relatively high energies. These effects are especially pronounced for incident energies ranging from 3 to 40 eV.

Finally the calculation procedure has been applied to obtain electron scattering cross sections in liquid Ar, confirming the tendency showed by the Ar clusters. Electron scattering cross sections in

liquids are required to model electron tracks in biologically relevant media for dosimetric purposes [16]. These results open the possibility of using the SCAR method to the scattering of electrons in molecular liquids, as water and other biomolecular systems.

## References

- [1] Ulrich B, Vredenborg A, Malakzadeh A, Schmidt L Ph H, Havermeier T, Meckel M, Cole K, Smolarski M, Chang Z, Jahnke T, and Dörner R 2011 *J. Phys. Chem. A* **115** 6936
- [2] Pérez de Tudela R, Márquez-Mijares M, González-Lezana T, Roncero O, Miret-Artés S, Delgado-Barrio G, and Villarreal P 2010 *J. Chem. Phys.* **132** 244303
- [3] Blanco F and García G 2002 *Phys. Lett. A* **295** 178
- [4] Blanco F and García G 2003 *Phys. Rev. A* **67** 022701
- [5] Blanco F and García G 2003 *Phys. Lett. A* **317** 458
- [6] Cowan R D 1981 *The Theory of Atomic Structure and Spectra* (London: University of California Press)
- [7] Riley M E and Truhlar D G 1975 *J. Chem. Phys.* **63** 2182
- [8] Zhang X Z, Sun J F, and Liu Y F 1992 *J. Phys. B* **25** 1893
- [9] Raju G G 2009 *IEEE Trans. Dielectrics and Electr. Insul.* **16** 1199
- [10] Staszewska G, Schwenke D W, Thirumalai D, and Truhlar D G 1983 *Phys. Rev. A* **28**, 2740
- [11] Zatsarinny O, Bartschat K, García G, Blanco F, Hargreaves L R, Jones D B, Murrie R, Brunton J R, Brunger M J, Hoshino M, and Buckman S J 2011 *Phys. Rev. A* **83**, 042702
- [12] Maljković J B, Milosavljević A R, Blanco F, Šević D, García G, and Marinković 2009 *Pys. Rev. A* **79** 052706
- [13] Blanco F and García G 2004 *Phys. Lett. A* **330** 230
- [14] Blanco F and García G 2009 *J. Phys. B* **42** 145203
- [15] Pflüger T, Senftleben, Ren X, Dorn A, and Ulrich J 2011 *Phys. Rev. Lett.* **107** 223201
- [16] Sanz A G, Fuss M C, Roldán A M, Blanco F, Limão-Vieira P, Brunger M J, Buckman S J and García G 2012 *Int. J. Radiat. Biol.* **88** 71